J. Phycol. **35,** 227–238 (1999)

SALINITY-DEPENDENT LIMITATION OF PHOTOSYNTHESIS AND OXYGEN EXCHANGE IN MICROBIAL MATS[1]

Ferran Garcia-Pichel,[2] *Michael Kühl,*[3] *Ulrich Nübel, and Gerard Muyzer*[4]

Max Planck Institut for Marine Microbiology, Celsiusstrasse 1, D-28359 Bremen, Germany

We used benthic flux chambers and microsensor profiling under standardized incubation conditions to compare the short-term (hours) and long-term (days) functional responses to salinity in eight different hypersaline microbial mats. The short-term response of productivity to changes in salinity was specific for each community and in accordance with optimal performance at the respective salinity of origin. This pattern was lost after long-term exposure to varying salinities when responses to salinity were found to approach a general pattern of decreasing photosynthesis and oxygen exchange capacity with increasing salinity. Exhaustive measurements of oxygen export in the light, oxygen consumption in the dark and gross photosynthesis indicated that a salinity-dependent limitation of all three parameters occurred. Maximal values for all three parameters decreased exponentially with increasing salinity; exponential decay rates (base 10) were around 4–5 $mL \cdot g^{-1}$. The values of mats in steady state with respect to salinity tended to approach this salinity-dependent limit. On the basis of environmental and ecophysiological data, we argue that this limitation was not caused directly by salinity effects on the microorganisms. Rather, the decreasing diffusive supply of O_2 in the dark and the increasing diffusion barriers to O_2 escape in the light, which intensify with increasing salinity, were likely responsible for the salinity-dependent limitations observed.

Key index words: **cyanobacteria; diatoms; hypersaline environments; microbial mats; photosynthesis; productivity; respiration**

Abbreviations: **AGP, areal gross photosynthesis; BBL, benthic boundary layer; BFC, benthic flux chamber; DC, O_2 consumption in the dark; DIC, dissolved inorganic carbon; DR, net flux of dissolved O_2 into a microbial mat; P, mat productivity in the light; VGP, volumetric gross photosynthesis**

Natural and man-made shallow hypersaline environments the world over harbor well-developed benthic microbial communities driven by the activities of phototrophic organisms, commonly in the form of microbial mats (Javor 1989). Hypersaline microbial mats serve as valuable models for the study of general biogeochemical processes (Des Marais 1995), provide insights for interpreting the geology of evaporites, and bear the keys to unravel the paleobiology of ancient stromatolitic fossils (Schopf and Klein 1992). The presence and activities of microbial mats influences the process of crystallization of salts in commercial salterns. Thus, understanding the biology of these communities, beyond advancing our knowledge of the functioning of intertidal areas and closed inland basins, where they constitute prominent ecological features (Javor 1989, Schultze et al. 1996, Alcorlo et al. 1997), has general, paleoenvironmental, and commercial implications.

With regard to primary producers, floristic accounts of hypersaline mats from diverse locations have revealed the overwhelming dominance of cyanobacteria and diatoms in these benthic communities and the presence of successive, distinct changes in community structure along salinity gradients, often displaying recurrent patterns among geographically distant sites (Felix and Rushforth 1979, Potts 1980, Bauld 1981, Jørgensen et al. 1983, Javor and Castenholz 1984, Ehrlich and Dor 1985, Gerdes et al. 1985, Giani et al. 1989, Mir et al. 1991, Zhang and Hoffmann 1992, Caumette et al. 1994). The commonality in patterns strongly suggests that salinity plays a determining role in shaping community structure in hypersaline mats. On the other hand, whereas several studies have dealt with the quantification of metabolic rates in these communities (Revsbech et al. 1983, Jørgensen and Cohen 1987, Canfield and Des Marais 1993), comparisons between studies are difficult, particularly with respect to measurements of oxygenic photosynthesis. Such enterprise is hampered by the widely divergent results obtained with different methodologies and by the dependence of benthic metabolism on physicochemical parameters as diverse as temperature, incident light, and flow velocity in the overlying waters, which make comparisons of rate measurements from different studies very uncertain. There exist indications that salinity may exert an influence on photosynthesis in microbial mats: an increase in mat productivity has been detected after an experimental salinity shift-down (Pinckney et al. 1995), and a decreasing trend of areal gross photosynthetic rates has been observed in a comparison of mats along a salinity gradient (Des Marais et al. 1989). We carried out exhaustive measurements of benthic gross pho-

[1] Received 9 July 1998. Accepted 21 November 1998.

[2] Author for reprint requests: e-mail fgarcia@mpi-bremen.de.

[3] Present address: Marine Biological Laboratory, University of Copenhagen, Strandpromenaden 5, 3000 Helsingør, Denmark.

[4] Present address: Netherlands Institute for Sea Research (NIOZ), P.O. Box 59, 1790 AB Den Burg (Texel), The Netherlands.

TABLE 1. Main characteristics of the benthic microbial mats.

Mat	Appearance	Dominant phototrophs	Field conditions		
			Salinity (%)	Water depth (m)	Origin
P2	soft, thin	cyanobacteria, diatoms	6	0.2–0.5	evaporation pond (side pool)
P3/4	compact	cyanobacteria, diatoms	6	0.5	evaporation pond
P4	leathery	cyanobacteria, diatoms	9	0.5	evaporation pond
P5	rubbery	cyanobacteria, diatoms	11	0.5	evaporation pond
P6	slimy, translucent	cyanobacteria	12	0.5	evaporation pond
NC2	soft, compact	cyanobacteria, diatoms	5–8	0.2–0.5	tidal channel
NC52	soft, compact	cyanobacteria, diatoms	5–8	0.2–0.5	tidal channel
NC3	leathery, hard	cyanobacteria	5–21	0.2–0.5	tidal channel

tosynthesis and oxygen exchange in the light and in the dark under standardized conditions on natural hypersaline environments submitted to various salinity conditions in order to establish the presence of any such generalized control of metabolic rates by salinity.

MATERIALS AND METHODS

The experiments were carried out during the second to fourth weeks of April 1996 and 1997 with benthic communities from the Ojo de Liebre Lagoon and the evaporating ponds of the saltern, Exportadora de Sal, S.A de C.V., in Guerrero Negro, Baja California Sur, Mexico. Detailed descriptions of these sites can be found elsewhere (Javor 1989, Des Marais 1995). A succinct description of the mats studied can be found in Table 1. The mats were diverse, differing in original salinity conditions, appearance, and community structure. All were dominated by cyanobacteria. Diatoms accounted for 0.1%–5% of oxygenic phototrophic cells. More than 30 different morphospecies and 16S rRNA gene sequences from oxygenic phototrophs could be identified in these mats. Detailed accounts on the biological diversity of oxygenic phototrophs within these mats is published elsewhere (Nübel et al. 1999). Pieces of microbial mats were excised and transported to our field laboratories, located in the town of Guerrero Negro, ca. 45 min drive from the field site. There, the samples were incubated in brines made up to the desired salinity (see below) by mixing filtered local brines from the salt works and, in some cases, deionized water obtained from a local reverse-osmosis facility. Salinity was determined with portable refractometers calibrated for NaCl brines (Cole Parmer, U.S.A.). Mats were incubated outdoors under natural illumination until analysis. Salinities are expressed as a percentage (weight of total salts per volume, $g \cdot 100\ mL^{-1}$).

Two sets of measurements were carried out. In the first set, each mat was incubated in brine made up to match the salinity of the respective field site at the time of collection (to within 0.5%), and measurements were started within 2–4 h. In this set we also measured the short-term (hours) responses of the mat communities to changes in the salinity of the overlying water. For this, each mat was submitted to two series of sequential shifts in salinity (one series for upshifts and one series for downshifts on separate pieces of mat), with measurements taking place at each shift after allowing the mats to reach short-term steady state with respect to O_2 exchange rates (usually within 2–3 h). In the second set of experiments, separate pieces of each mat were incubated at different salinities (3%, 9%, 13%, 18%, and 23%) for 5 days (4 days in one case) in outdoor flumes. Brines of the desired salinity were circulated in the flumes by means of submersible aquarium pumps and returned to a reservoir, where they were aerated. The reservoirs were shaded from sunlight so that the brines did not heat up excessively. Salinity of the brines was monitored during the incubation period and corrected for evaporative losses by additions of freshwater. Maximal deviation in salinity during incubation amounted to 0.5%.

Measurements of bulk oxygen exchange. Bulk O_2 exchange was measured with benthic flux chambers (BFC) under standard conditions of stirring, illumination, and temperature. Each BFC consisted of an inverted glass bell jar with an opening at the top and containing a hanging magnetic stirring bar. The top opening was closed air-tight with a rubber stopper, through which an outlet syringe needle and a Clark-type microelectrode were inserted. A motorized external magnet drove the inner stirring bar. The syringe outlet was used to fill the chambers by suction, and to empty them as needed. The microelectrode monitored O_2 partial pressure in the chambers. In light incubations, a standard illumination of ca. 800 μmol photons$\cdot m^2 \cdot s^{-1}$ (400–700 nm, scalar irradiance), as measured with a quantum scalar irradiance meter (Biospherical Instruments, QSL-100), was provided by a halogen fiber optic illuminator (Schott KL1500) equipped with collimating lenses. Microelectrode readings were linearly calibrated from readings in air-saturated and N_2-flushed brines. Calibrated electrode readings in 100% air saturation were converted to molar units by Winkler titrations of air-saturated brines. Incubation temperatures could only be partially controlled, varying maximally between 21.3° and 24.7° C (mean = 23.2° C, SD = 1.09° C). Two chambers were used simultaneously for each treatment. For incubations in light, the measurements were carried out in triplicate (sometimes in duplicate only), yielding a total of six rate measurements per condition. In dark incubations, measurements were only duplicated. Each chamber determined average rates over ca. 20 cm^2 of mat surface. The O_2 exchange rate under standard illumination is equated hereafter to the mat productivity in the light (P), which bears a positive sign when it corresponds to a net export of O_2 from the mat. The O_2 consumption in the dark (DC) cannot be directly equated to aerobic respiration, because chemical and biological sulfide oxidation may be responsible for an undetermined proportion of this rate; O_2 consumption in the dark bears a negative sign, as it corresponds to a net import into the mat.

Microelectrode measurements. In similar setups and in parallel to the measurements with the benthic exchange chambers, we measured profiles of O_2 concentration within and above the mats under standard illumination and flow conditions, using O_2 microelectrodes, custom-made according to Revsbech (1989), with tip diameters of 5–10 μm, average 90% response times of <0.5 s, and stirring sensitivity of <2%. A two-point calibration of the microelectrodes at each salinity was carried out using electrode readings in fully aerated brine (100% saturation) and in the anoxic, deep layers of the mats (zero). In the measuring setup, mats were incubated under a flow of aerated brine in small flumes (Lorenzen et al. 1995) and microelectrodes were positioned with a motorized micromanipulator (Märtzhäuser, Germany). All microsensor work was monitored by observation through a binocular microscope. Data acquisition and microelectrode positioning were computer controlled using a custom-made program (B.M. Bebout and V. Meyer, unpubl.). From the slopes of O_2 concentration in the benthic boundary layer over the mats and the diffusion coefficient for O_2 in the respective brines, mat productivity in the light (P) and oxygen consumption in the dark (DC) could be obtained (Garcia-Pichel and Belnap 1996, Kühl et al. 1996). The diffusion coefficient for O_2 as a function of salinity was calculated after Li and Gregory (1974). Profiles of volumetric gross photosynthesis (VGP) at 100-μm intervals (200 μm for mat P6)

TABLE 2. Parameters measured and derived in benthic phototrophic communities (mats). M, mass or molar amount of oxygen; L, length; T, time.

Parameter	Abbreviation	Definition	Dimensions	Measuring techniques
Productivity	P	flux of oxygen between mat and bulk water in the light	$M \cdot L^{-2} \cdot T^{-1}$	BFC, oxygen profiling
Dark O_2 consumption	DC	flux of oxygen between mat and bulk water in the dark	$M \cdot L^{-2} \cdot T^{-1}$	BFC, oxygen profiling
Volumetric gross photosynthesis	VGP	rate of oxygen evolution within a unit volume of mat	$M \cdot L^{-3} \cdot T^{-1}$	Microsensor (Light-Dark-shift method)
Areal gross photosynthesis	AGP	rate of oxygen evolution below a unit area of mat	$M \cdot L^{-2} \cdot T^{-1}$	AGP is the integral sum of all measured VGPs in the photic zone

within the photic zone of the mats were done with the light–dark shift method (Revsbech and Jørgensen 1983), limiting data acquisition to the first 2 s after darkening.

Parameters measured and derived. The parameters measured and derived, together with units, measuring techniques and other relevant characteristics have been gathered in Table 2. The two techniques used offer distinct advantages and disadvantages and allow measurement of different parameters with different resolutions. BFCs measure fluxes between the water and the mats, either P or DC, which are both a result of the combined rates of metabolic and/or chemical processes involving O_2 and, thus, are secondary parameters. The absolute values of P and DC measured with BFCs are sensitive to the hydrodynamic regime in the chambers, which is a function of the shape of the chambers, of the stirring velocity within them, and of the microtopography of type of mat investigated. BFCs offer a large integrating area compared to that measured by microelectrodes, yielding estimates that average possible microheterogeneities in the horizontal dimension.

Microelectrode profiling offers the advantage that it measures, in addition to P and DC, direct estimates of gross photosynthetic rate (oxygen evolution) within a certain volume of mat (VGP), a primary parameter, and they offer information on the distribution of metabolic rates in the vertical dimension, z, at high spatial resolution. Other parameters, such as the depth-integrated value for VGP (areal gross photosynthesis, AGP) or the respiration in the light can be computed or modeled from the O_2 concentration profiles and the VGP (z) measurements (Kühl et al. 1996). Because of their small size, however, spatial heterogeneity in the horizontal dimension is not taken into account, unless time-consuming multiple sampling is carried out, and thus the goodness of the estimates is unknown. Repeatedly measuring concentration profiles at the same point in the mat under varying environmental conditions yields perfectly valid results for comparative purposes, provided the mat is not irreversibly disturbed by sampling. As with BFCs, the hydrodynamics of the overlying water will influence some parameters like mat P and DC, and in addition, the hydrodynamic effects of introducing the electrode in the water flow may induce biases in the absolute values measured (Lorenzen et al. 1995).

However, most of these problems associated with either technique are irrelevant for comparative purposes, as long as the possible biases are kept constant and do not vary systematically with sample structure and salinity. Thus, it is legitimate to compare mat productivity in the light and oxygen consumption in the dark in different communities if the measuring set-up imposes the same conditions of light, flow, and temperature, as was the case in all BFC measurements and in all microsensor measurements. It is inappropriate to compare microsensor and BFC measurements, because the hydrodynamics associated with each technique are hard to match; yet any comparative trends among mats should be revealed by both types of techniques. An effort was made to obtain complete BFC and O_2-profiling data sets in the short-term incubation experiments. For the long-term incubations, where experimental design imposed using many different mat pieces, VGP profiles could only be measured in two mat types.

RESULTS

Short-term incubations. When incubated under salinities similar to those found in the field, the O_2 export rate in the light (P), which is a measure of productivity, varied widely among mats; the variation ranged from 1 (mat NC3 at 16% salts) to 6 mmol $O_2 \cdot m^{-2} \cdot h^{-1}$ (mat P2 at 6% salts). In mat P6, however, variation between two separate mat pieces was twofold, indicating substantial horizontal heterogeneity at the scale of square decimeters in this mat. A trend in P at field salinity could be observed: highest rates corresponded to lower original salinities. Des Marais et al. (1989), had observed a similar trend in areal gross photosynthesis. Dark O_2 consumption (DC) in incubations at field salinity was more conservative than P among mats, varying roughly between 1 and 3 mmol $O_2 \cdot m^{-2} \cdot h^{-1}$. These data, as well as the response of both P and DC to short-term changes in salinity are presented in Figure 1. It is evident that P presented an optimum close to the original field salinity in all mats, although in some cases a small increase in P could result from a decrease in salinity. The behavior of P with respect to experimental variations in salinity was markedly divergent among mats, so that, for example, P in mat P4 was very sensitive to both increases and decreases in salinity, whereas P in mat NC3 was remarkably resilient to changes in either direction. DC did not vary in concordance with P, and in general, DC decreased in magnitude with increasing salinity regardless of the mat. Only mat P4 yielded a DC vs. salinity curve with a relative maximum.

Oxygen profiling yielded generally higher absolute values of P than BFCs, but the responses of P to salinity changes as determined with O_2 profiling were congruent with those determined with BFCs: some mat communities showed clear maxima (P4) and some showed flatter responses (NC3). Areal gross photosynthesis (AGP) in these communities, however, was related to salinity changes in a much less community-specific fashion, and all mats displayed decreasing AGP rates with increasing salinity (Fig. 2). This discrepancy between AGP and P in the same mat points to factors such as respiration in the

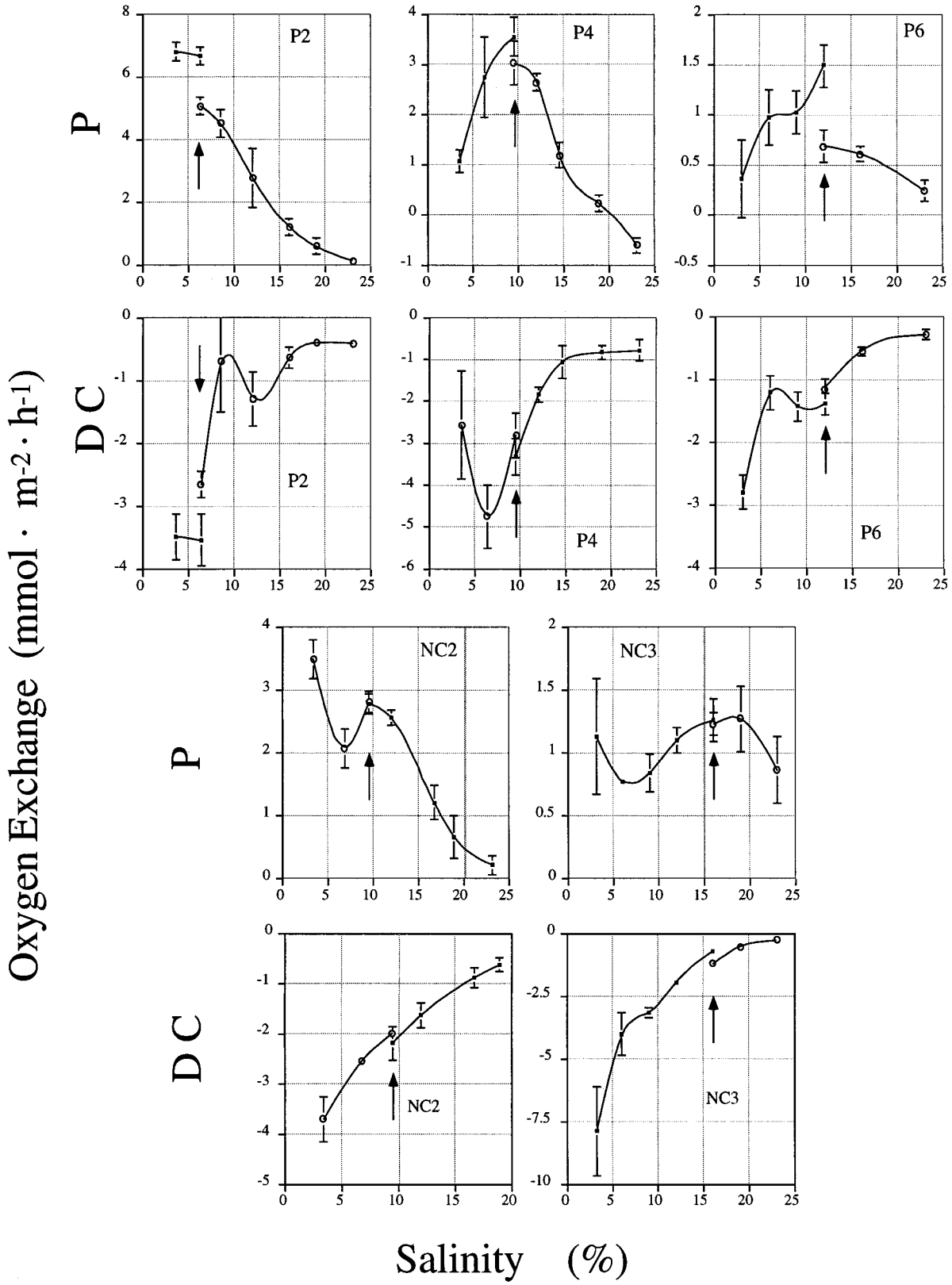

FIG. 1. Oxygen exchange rates measured in the light (P, productivity, measured at an irradiance of 800 μmol photon·m^{-2}·s^{-1}) and in the dark (DC, dark O_2 consumption) with BFCs, and the effect of short-term changes in salinity on both parameters in mats P2, P4, P6, NC2, and NC3. Two series of measurements are plotted for each mat, corresponding to a series of upshifts and a series of downshifts in salinity, measured in separate mat pieces. Arrows indicate the initial salinity of the measurements, which corresponds approximately to the salinity to which each mat was exposed under natural conditions in the field. Bars indicate ±SD based on four to six replicate measurements per point.

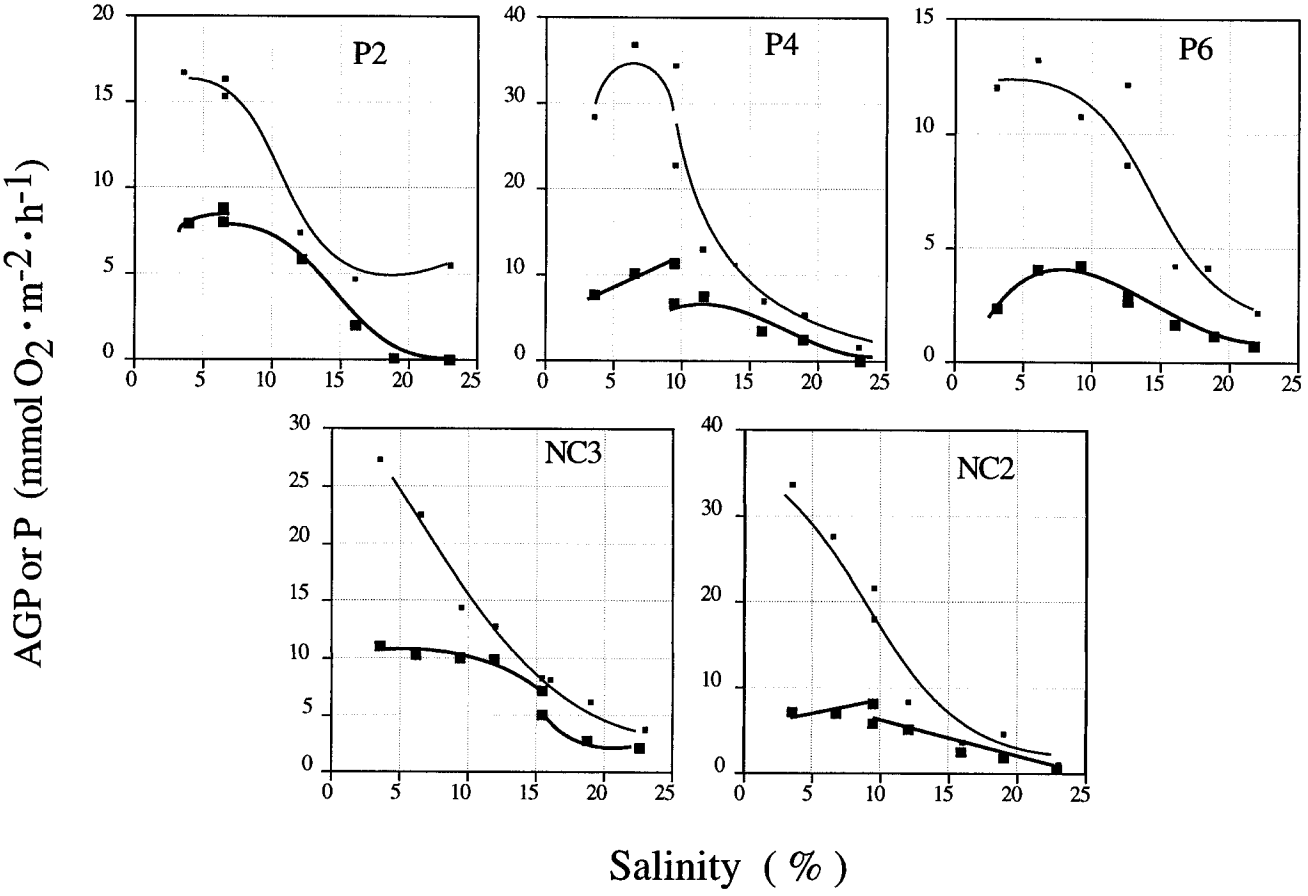

FIG. 2. Productivity (P, large symbols) and areal gross photosynthesis (AGP, small symbols) measured by microsensor profiling of oxygen concentration and volumetric gross photosynthesis (VGP), as a function of salinity in mats P2, P4, P6, NC2, and NC3; data are from short-term acclimation experiments.

light and light-coupled respiration as important players in determining the overall short-term response to salinity changes of the mat communities. Respiration in the light must become increasingly important at low salinities, where the differences are higher. In other words, the decreases in productivity measured at high salinity can be directly traced to decreases in gross photosynthetic rates, but the decreases in P at low salinity seem to be strongly dependent on an increased respiration in the light.

Long-term incubations. Measurements obtained for P and DC after long-term (4–5 days) incubation under different salinities are presented in Figure 3. The responses of P and DC in the various mats converged into a much more homogeneous pattern: all mats displayed decreasing fluxes of O_2 both in the light and in the dark with increasing salinity regardless of their original conditions. Traces of the optimum-bearing responses observed in the short-term incubations were only found in mat P6, the only one not to show a statistically significant maximum of P at the lowest salinity.

Generalized relationships between salinity and functional parameters. The experiments described point to a certain dependence between some functional parameters of the mats, P in particular, and salinity. In order to obtain a better picture of this, we have plotted in Figure 4 the distributions of values of mat productivity in the light (P) obtained during the work as a function of the salinity at which they were measured. For each salinity, the distribution of values was normal. The plot reveals that, when all experiments are taken into consideration (Fig. 4A), salinity alone does not allow the prediction of P values but that it does impose an apparent upper limit to P. This apparent limit to P sets in above seawater salinities and decays with salt concentration of the brines in an exponential fashion (apparent exponential decay rates were 0.043–0.047 [% salts]$^{-1}$, or 4.3–4.7 mL·g^{-1}). When only those data obtained in mats in steady state (incubated 4 days or more at a certain salinity) are taken into account, the upper limit remains, and the values tend to approach this limit, so that salinity does not only impose an apparent upper limit to P but becomes a much better predictor of P as well. An alternative way of describing this phenomenon is that the means of the data distributions decrease with salinity. This salinity-dependent limitation was not restricted to P but also applied to DC (Fig. 4C). In the case of DC, the ap-

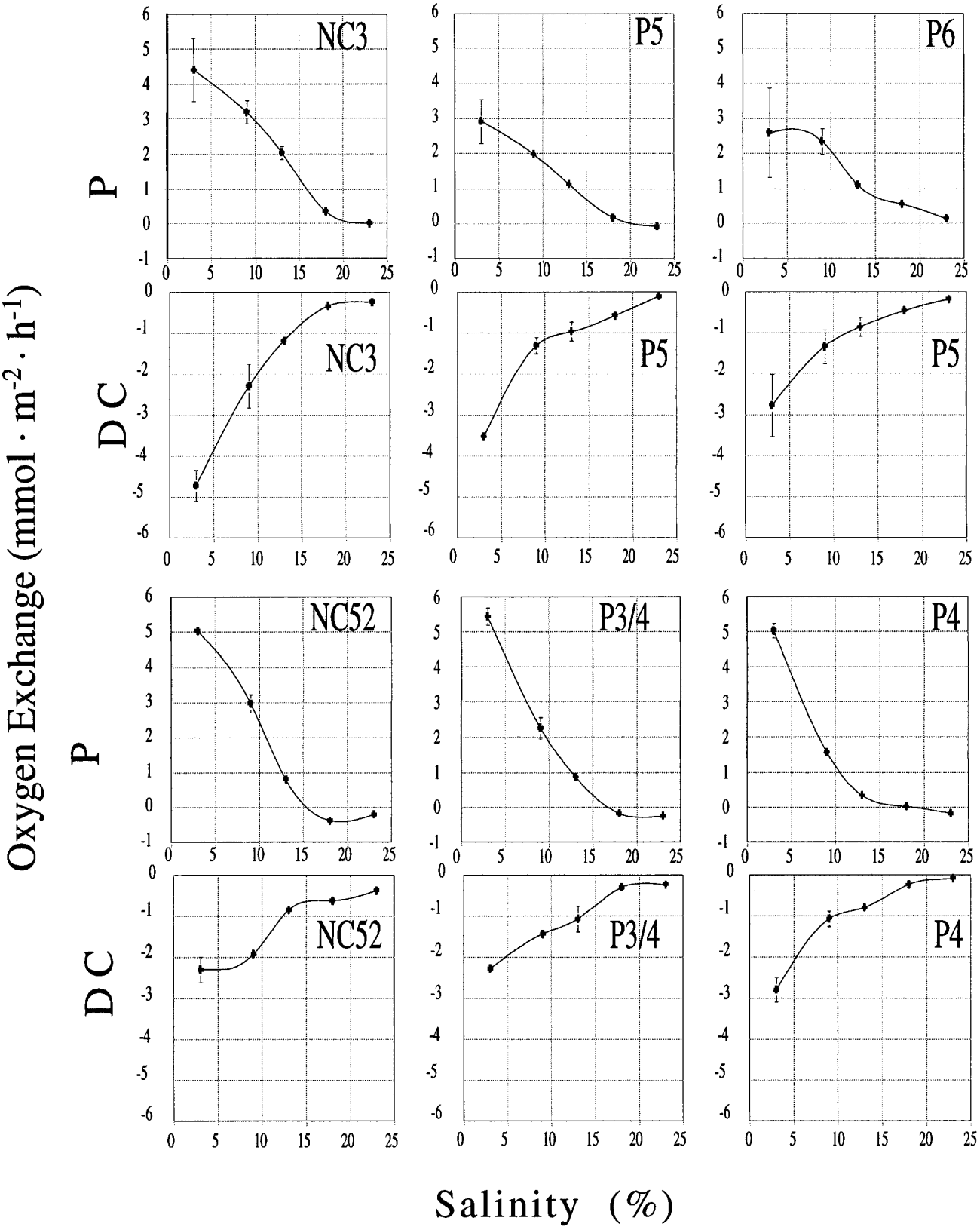

FIG. 3. Oxygen exchange rates measured in the light (P, productivity in the light, measured at an irradiance of 800 μmol photons·m^{-2}·s^{-1}) and in the dark (DC, dark O_2 consumption) with BFCs, and the effect of long-term changes in salinity on both parameters in mats P3/4, P4, P5, P6, NC52, and NC3. The data correspond to pieces of mat incubated during 5 days (4 days for NC3) at the corresponding salinity. Bars indicate ±SD based on four to six replicate measurements per point.

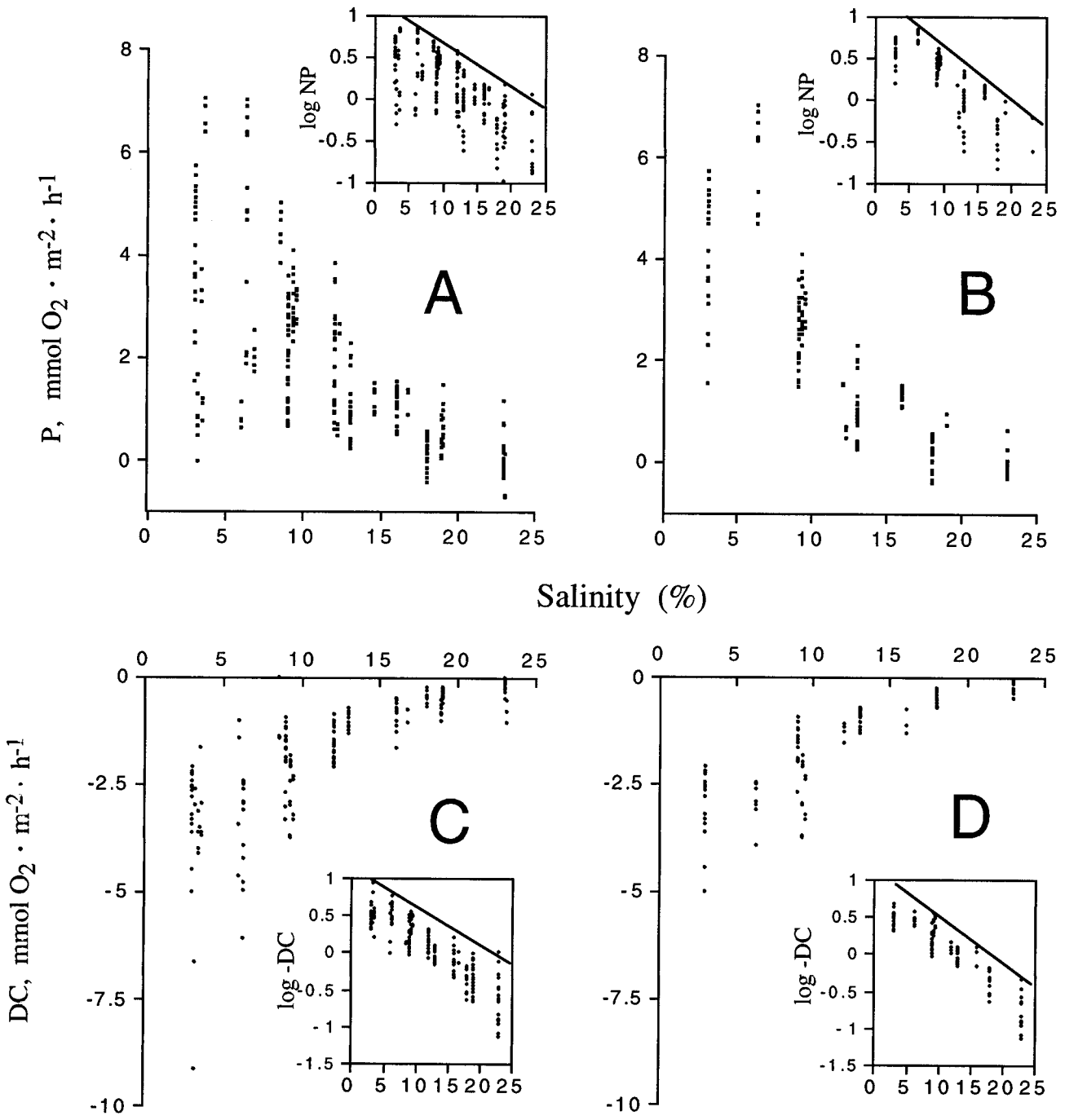

FIG. 4. General plots of oxygen exchange vs. salinity. (A, B) Rates of net productivity in the light (P, measured at an irradiance of 800 μmol photons·m^{-2}·s^{-1}) as a function of salinity. (C, D) Rates of dark O_2 consumption (DC) as a function of salinity. Panels (A) and (C) include all single measurements carried out in mats P2, P3/4, P4, P5, P6, NC2, NC52, and NC3, after both short-term and long-term incubations. Panels (B) and (D) contain only those data measured under steady-state conditions of salinity of more than 4 days. Inserts show log-transformed absolute rates versus salinity under exclusion of zero values.

parent limit to *absolute* values decays exponentially with a rate of 4.3–4.6 mL·g^{-1}. Restricting measurements of DC values to mats in steady state with respect to salinity (Fig. 4D) improves the predictive power of salinity for DC, but not as clearly as for P.

The distribution with salinity of VGP measured in these mats at all depths within them is plotted in Figure 5A. It is apparent from this figure that a similar salinity-dependent upper limitation of VGP rates occurred. The limit decays exponentially with rates of 4.5–5 mL·g^{-1}. The abundance of low values in VGP throughout the salinity range (the frequency distributions of the data at each salinity decreased in a log-linear fashion) stems from measurements

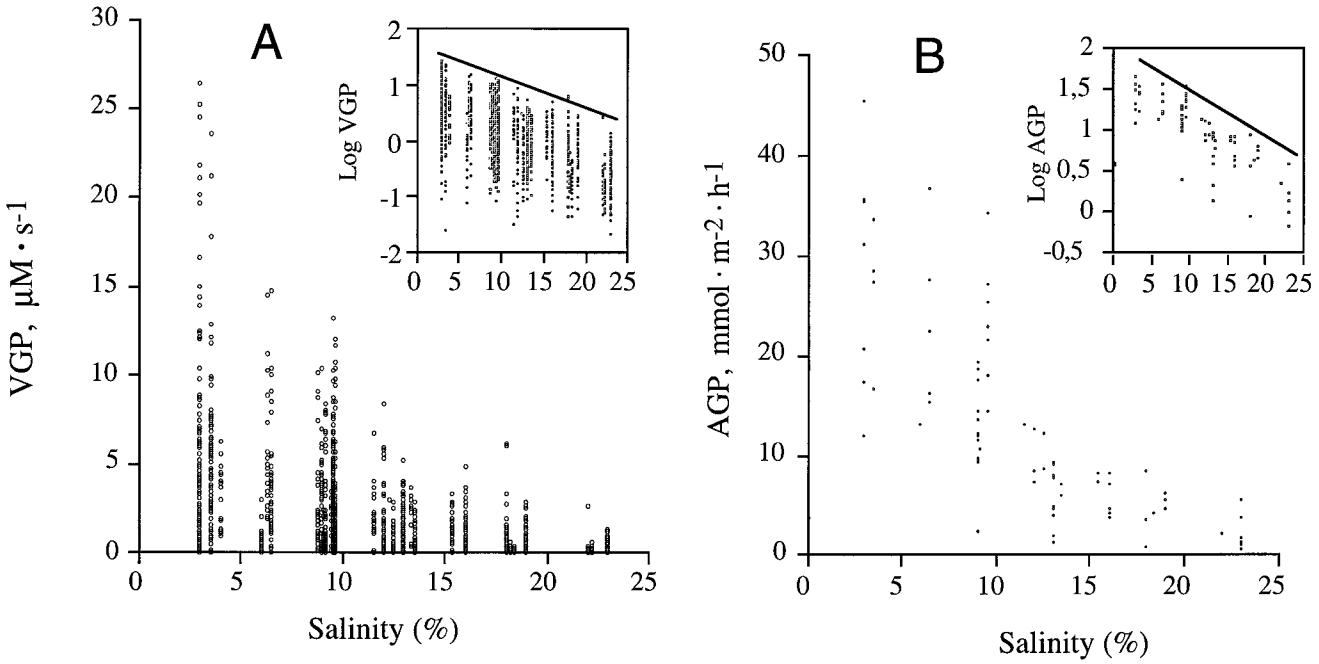

FIG. 5. General plot of the rates of volumetric gross photosynthesis (VGP, A) and computed rates of areal gross photosynthesis (AGP, B) as a function of salinity. Included are data for mats P2, P4, P5, P6, NC2, NC52, and NC3 incubated at an irradiance of 800 μmol photons·m^{-2}·s^{-1} and data from both steady-state and salinity shifts. Inserts show log-transformed data versus salinity.

carried out deep within the photic zones of the mat where VGP is obviously light limited. Figure 5B shows the distribution with salinity of the depth-integrated values of AGP for each mat and condition available. Although the number of data points is restricted, the data are consistent with a salinity-dependent limitation of AGP as well, where the exponential decay rates are around 5 mL·g^{-1}.

DISCUSSION

The salinity-dependent limitation of metabolic parameters in hypersaline microbial mats seems apparent and pervasive from the data presented, involving primary (VGP), derived (AGP), and secondary (DC, P) parameters. Moreover, the uniformity in the exponential relationship between the upper limits of the parameters measured and salinity is intriguing. The finding that the rates tend to approach this limit from below in steady state indicates that, in the absence of environmental disturbances, salinity strongly controls metabolic functions in these communities.

Only in a few other instances have such clear-cut limitations of metabolic activity by physicochemical parameters been demonstrated. The case of salinity is not simple, and several interpretations might be possible. The simplest explanation may invoke a putative metabolic burden of excess solutes (or lack of free water) on the microorganisms, so that metabolic rates are depressed. The burden should increase with increasing salinity, such that the rate depression increases with salinity as well. This mechanism has been invoked to explain the increase in photosynthesis measured after a decrease in salinity in certain microbial mats (Pinckney et al. 1995). However, the nature of the putative metabolic burden is unknown and cannot be immediately deduced from physiological studies available on the acclimation of microorganisms to osmotic stress. Two types of evolutionary adaptations to salt stress are known to be reflected in the so-called *salt-in* and *salt-out* cells types (Galinsky 1995). Salt-in organisms (typically restricted to halophilic Archaea) allow salts to enter the cells so that they are isoosmotic with their surroundings. All structural and enzymatic proteins have evolved to be fully functional under such conditions, and they do not function at low ionic strength (Danson and Hough 1997). Thus, no specific metabolic burden can be identified in these types of cells at high salinity; if any condition limits metabolism, then it is low salinity. Salt-out organisms, like the cyanobacteria and diatoms that form the trophic basis of the ecosystems described in this study, actively extrude salt from their cytoplasm (usually also exchanging Na^+ by K^+) and attain isoosmotic conditions with their environment by synthesizing and accumulating organic-compatible solutes (Joset et al. 1996). Salt extrusion may impose a metabolic burden on the cells that may translate into increased respiration rates at high salinity, which in turn would require increased oxygen consumption in the dark (DC) with increasing salinity. This adaptive mechanism fails to explain our experimental observations. The synthesis of osmolites represents a relocation of the fixed carbon and an increase of the total carbon per cell but does not nec-

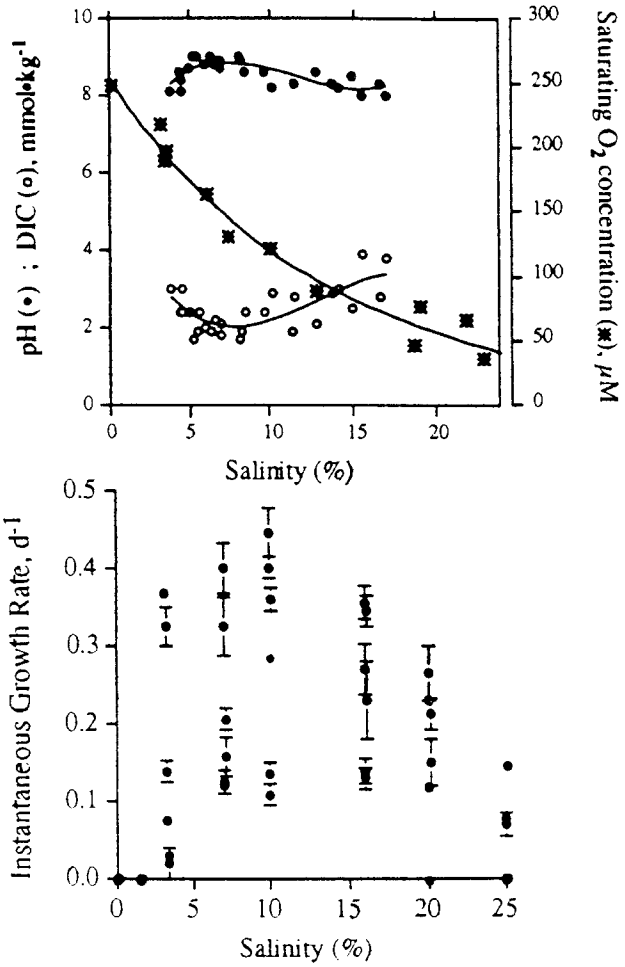

FIG. 6. Variation with salinity of parameters relevant for the discussion of results. Upper panel: chemical characteristics of Guerrero Negro brines. For the concentration of oxygen at air saturation, each point is the mean of triplicate measurements. Values of pH and DIC are from Des Marais et al. (1989). Lower panel: pooled growth rates attained in artificial marine brines (dilute batch cultures) under standard temperature and illumination by six different strains of extremely halotolerant cyanobacteria. Data are from Garcia-Pichel et al. (1998).

essarily affect the rates of O_2 evolution or uptake. From studies on halotolerant phototrophs, there is no evidence for an exponential salinity-dependent upper limit to growth in dilute batch cultures. Rather, each strain displays good growth within a certain salinity range, where physiological adaptation is possible, and growth is severely depressed when salinity exceeds the upper limit of this range (Fig. 6). In addition, the responses of AGP that we observed (e.g. a generalized increase when salinity was decreased), happened within hours of incubation. This is probably too short a time to attribute the responses to physiological acclimation processes, which in culture, could take days (Vonschak et al. 1988). In summary, the results obtained in this study cannot readily be explained on the basis of known physiological responses to salt and constitute an apparent paradox.

As an alternative explanation for salinity-dependent limitations, one can postulate that the effects of salinity may not be direct but may result from changes in other physicochemical parameters of brines that covary with salt content. Ionic composition and pH change as salinity increases. Specific gravity, surface tension, specific heat, viscosity, and conductance increase, while gas solubility, gas diffusion coefficients, and water activity decrease with increasing salinity (Javor 1989: table 1.3.). Of obvious importance to metabolic activities such as oxygenic photosynthesis and respiration is the decrease in the capacity of aqueous solutions to hold gases as salinity increases; the brines become saturated at lower molar concentrations. For the case of NaCl brines in equilibrium with air at standard atmospheric pressure, for example, the molar concentration of O_2 required for saturation decays exponentially with salinity (base 10 decay constants of 2.8 $mL \cdot g^{-1}$; Sherwood et al. 1991). In our experimental seawater brines, this dependency was well described by decay constants around 3–4 $mL \cdot g^{-1}$ (Fig. 6).

It is, in fact, possible to explain the effects of salinity on DC as an indirect effect of salinity on various physicochemical parameters. The net flux of dissolved O_2 into the mat (DR) is dependent on diffusive transport from overlying waters through the benthic boundary layer (BBL). The vertical diffusive O_2 flux, J, through the BBL with an effective thickness, Z_δ, under the assumption of negligible consumption rates within it is described by Fick's first law of diffusion as

$$J = D(C^* - C_0)/Z_\delta \quad (1)$$

where D is the molecular diffusion coefficient, C* is the concentration in the bulk water (air saturation), and C_0 is the concentration at the surface of the mat (Jørgensen and Des Marais 1990). Maximal possible fluxes occur when $C_0 = 0$; that is, when respiration rates are so high that all incoming O_2 is consumed at the surface of the mat. Because D, C*, and Z_δ are all a function of salinity (s) the maximal fluxes (J_{max}) will be given by

$$J_{max}(s) = D(s)C^*(s)/Z_\delta(s). \quad (2)$$

D(s) can be derived from the formulas given by Li and Gregory (1974), and C*(s) was determined experimentally during our work. Only the function $Z_\delta(s)$ is unknown. But for flows occurring over a planar surface, Z_δ is known to vary according to the expression

$$Z_\partial = 5\left(A\frac{\mu}{\rho}\right)^{1/2}, \quad (3)$$

where A is a factor inversely proportional to flow velocity of the liquid and directly proportional to the dimensions of the surface, μ is the dynamic vis-

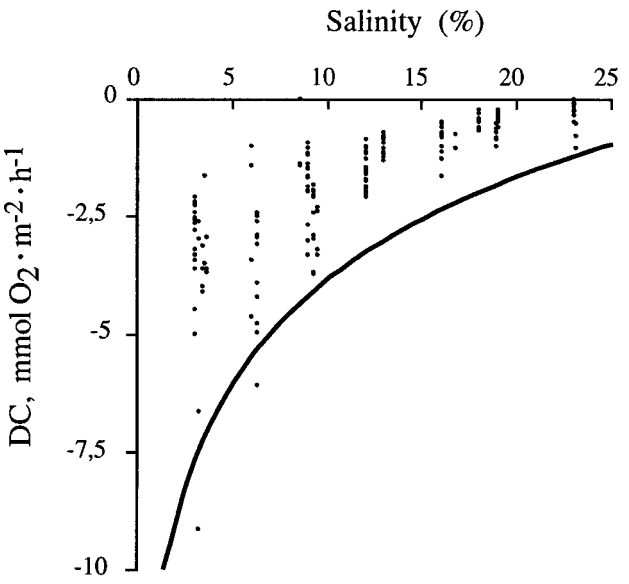

FIG. 7. Theoretically maximal DR rates with salinity (line) according to a simple diffusion model (see text) circumscribed the distribution of measured DR values.

cosity, and ρ the density of the flowing liquid (Jørgensen and Revsbech 1985, Vogel 1989). We determined relative changes in Z_δ with salinity by fixing arbitrarily Z_δ to 200 μm at s = 3% (in concordance with our O_2 profiles) and using values of ρ(s) and μ(s) from Riley (1975). One can calculate an increase of Z_δ to 224 μm at 200% salinity. Calculations of $J_{max}(s)$ according to equation 2, assuming Z_δ at 3% salinity of 200 μm, T = 20° C, yield the function depicted in Figure 7. This function fits an exponential decay of J_{max} with salinity, with decay rates of 4 $mL \cdot g^{-1}$; it circumscribes well the apparent limitation of DC obtained in the experimental part. Thus, the observed limitations of DC with increasing salinity can be explained solely on the basis of increasing diffusion limitation due to decreasing O_2 solubility.

An explanation for the observed salinity-dependent limitation of P (and of AGP) on the basis of increasing diffusion limitation might not be as straightforward as in the case of DC. On the one hand, it is possible that the net influx of CO_2 into the mat suffers from diffusion limitations. On the other hand, it is known that microalgae in general and cyanobacteria in particular develop efficient carbon concentration mechanisms that allow for the transport of bicarbonate ions into the cells making photosynthesis dependent on dissolved inorganic carbon (DIC) rather that CO_2 partial pressure (Raven 1991). The possible effects of salinity on benthic photosynthesis through availability of carbon needs to take into account not only the salinity dependence of CO_2 solubility in brines, but also the salinity effects on the entire carbonate system. Two independent lines of evidence suggest that carbon limitation does not play an important role in the observed phenomenon. First, CO_2 can be made available to the oxygenic phototrophs from within the mat as a result of internal respiratory processes, and because, in the light, O_2 evolution within the mat increases the potential for respiration, there is no reason to expect that limitations due to shortage of CO_2 should limit the rates of gross photosynthesis (either areal or volumetric) at high salinity. In other words, DIC diffusion from the bulk water may play a role in limiting mat productivity in the light (P) under steady-state conditions, but that does not preclude fast inorganic carbon recycling within the community, which would allow for high gross rates of photosynthesis and respiration in the light. Furthermore, under non-steady-state conditions, P may temporarily be high at high salinity due to a ''surplus'' of internally produced CO_2. Yet the limitations observed in our study involved both gross and net photosynthetic rates and included steady-state and non-steady-state measurements. A second line of evidence suggesting that CO_2 does not play a major role in the salinity-dependent limitations observed stems from direct measurements of DIC in the brines of Guerrero Negro (Des Marais et al. 1989, Fig. 6); DIC does not show a decreasing trend with salinity. Hence, factors other than DIC availability must be responsible for the salinity-dependent limitation of photosynthesis. For example, elevated O_2 tensions may have a negative effect on photosynthesis because O_2 acts as a competitive inhibitor of RubisCO carboxylase activity (Raven 1991) and because they result in photooxidation in mats (Garcia-Pichel and Castenholz 1994). In cultures, cyanobacteria display decreased growth rates under elevated O_2 tensions (Márquez et al. 1995). In our system, as salinity increases, saturation of O_2 is reached at lower molar O_2 concentrations. Thus, any putative negative effects of elevated O_2 partial pressure on photosynthetic activity will be noticeable at lower photosynthetic rates as salinity increases. This point is illustrated in Figure 8 using data obtained from mat P4. Our data are congruent with the operation of such an inhibitory mechanism. High and relatively stable partial pressures of oxygen were measured not only in P4 but in all mats.

In order to assess the magnitude of the effect of salinity on the O_2 accumulations, we applied a simple diffusion-reaction model for the formation of oxygen gradients in benthic phototrophic communities (Epping 1996, data not shown). We included environmental conditions (temperature, diffusion coefficients, volumetric rates of photosynthesis, and respiration) typically associated with the mats, imposed the condition that AGP should remain invariant throughout the salinity range of 3%–23%, and modeled the oxygen concentration profiles. The results indicate that for AGP rates resulting in maximal O_2 partial pressures of 1 atm at 3% salinity within the community (a typical condition in benthic microbial mats), one should expect maximal O_2

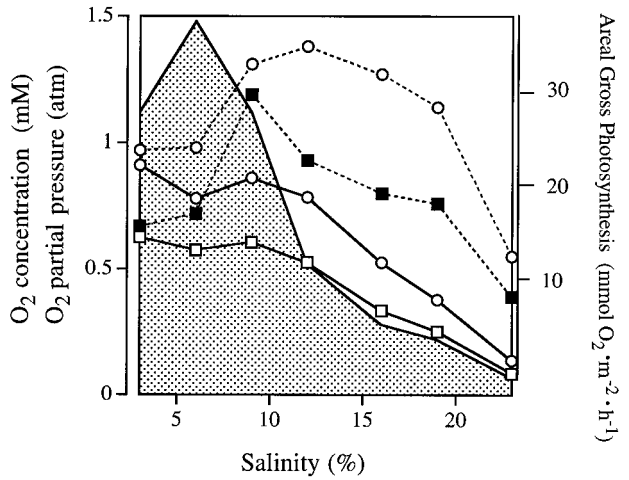

FIG. 8. Effect of salinity in short-term incubation experiments on the areal gross photosynthesis (AGP) and on the oxygenation of the photosynthetically active layer (0–2 mm) in mat P4 as obtained from microsensor oxygen profiling (profiles not shown). Legend: shaded area depicts AGP, broken lines depict partial pressures of O_2, solid lines depict molar O_2 concentrations; Empty circles refer to maximal values attained within the photosynthetically active layer, and solid squares refer to average values integrated along it. As salinity increased, the areal gross photosynthesis and the molar oxygenation of the photic zone decreased in such a way that the partial pressure of oxygen in the mat remained relatively constant up to a salinity of 19%.

partial pressures of 2 atm at 15% salts and 4 atm at 23% salinity; these O_2 partial pressures could result in structural damage to the community and are unlikely to be ever reached.

A full explanation for the limiting effect of salinity on photosynthetic rates in benthic microbial communities is not possible at this point and necessitates further investigations. Interpretations based on the indirect effects of salinity on O_2 solubility can explain the limitations observed, the magnitude of their dependence on salinity, and the short time frames within which some of the changes are observed. Our hypothesis lends itself to empirical testing as it predicts that limitations can be lifted if the O_2 accumulations can be prevented. This implies that planktonic communities of low cell density should not be submitted to similar salinity-dependent limitations. Experiments are in progress to test this hypothesis. Such an indirect effect of salinity may offer explanations as to why mats at the upper range of salinity are usually embedded in slime, less compact, and less densely colonized, since this should result in much less strong accumulations of oxygen.

The findings that we present have obvious and important implications for the ecology of hypersaline bodies of water. It can be predicted that the turnover times for carbon, the regeneration times after episodic catastrophic events, and the resilience of these communities to changes in environmental factors other than salinity must decrease with salinity as metabolic rates slow down. Salinity control of productivity may override other (nutrient) limitations under hypersaline conditions. The presence of this salinity-dependent limitation may also explain why benthic communities become restricted at salinities above 18% salt, even though some cyanobacteria can grow well (in culture) at salinities well above that level (Brock 1976, Yopp et al. 1978, Garcia-Pichel et al. 1998). The salinity-dependent limitations described here may enable the use of indicator fossil microalgae (i.e. Wilson et al. 1996) for paleoecological reconstructions of benthic productivity.

We also realize that the effects described in this contribution represent, in a certain way, the salinity-dependent intensification of diffusive limitations that must operate in benthic communities, at large, under any conditions. In the future it should prove interesting to assess the possible impact of this theoretical diffusion limitation to benthic metabolism.

We are indebted to A. Eggers and V. Hübner for invaluable technical assistance. The continued logistic support of Exportadora de Sal, S.A. de C.V., BCS, Mexico, is greatly appreciated. We also thank B. M. Bebout and V. Meyer for developing the data acquisition hardware and software and E. Epping for help with the diffusion-reaction model. This research was supported by the Deutsche Forschungsgemeinschaft and the Max-Plack Society.

Alcorlo, P., Diaz, P., Lacalle, J., Baltanas, A., Florin, M, Guerrero, M. C. & Montes, C. 1997. Sediment features, primary producers and food web structures of two shallow temporary lakes (Monegros, Spain). *Water Air Soil Pollut.* 99:681–8.

Bauld, J. 1981. Occurrence of microbial mats in saline lakes. *Hydrobiologia* 81:87–111.

Brock, T. D. 1976. Halophilic blue-green algae. *Arch. Microbiol.* 107:109–11.

Canfield, D. E. & Des Marais, D. J. 1993. Biochemical cycles of carbon, sulfur and free oxygen in a microbial mat. *Geochim. Cosmochim. Acta* 57:3971–84.

Caumette, P., Matheron, R., Raymond, N. & Rexans, J. C. 1994. Microbial mats in hypersaline ponds of the Mediterranean salterns (Salins-de-Giraud, France). *FEMS Microbiol. Ecol.* 13: 273–86.

Danson, M. J. & Hough, D. W. 1997. The structural basis of protein halophilicity. *Comp. Biochem. Physiol.* 117:307–12.

Des Marais, D. J. 1995. The biogeochemistry of hypersaline microbial mats. *Adv. Microb. Ecol.* 14:251–72.

Des Marais, D. J., Cohen. Y., Nguyen, H., Cheatham, M. & Munoz, E. 1989. Carbon isotopic trends in the hypersaline ponds and microbial mats at Guerrero Negro, Baja California Sur, Mexico: implications for Precambrian stromatolites. *In* Cohen, Y. & Rosenberg, E. [Eds.]. *Microbial Mats. Physiological Ecology of Benthic Microbial Communities.* American Society for Microbiology, Washington, D.C., pp. 191–203.

Ehrlich, A. & Dor, I. 1985. Photosynthetic microorganisms of the Gavish Sabkha. *In* Friedmann, G. M. & Krumbein, W. E. [Eds.] *Hypersaline Ecosystems. The Gavish Sabkha,* Springer Verlag, Heidelberg, pp. 296–321.

Epping, E. H. G. 1996. Benthic phototrophic communities and the sediment–water exchange of oxygen, Mn(II), Fe(II), and silicic acid. Ph.D. thesis, University of Groningen, Groningen, The Netherlands, 222 pp.

Felix, E. A. & Rushforth, S. R. 1979. The algal flora of the Great Salt Lake, Utah, U.S.A. *Nova Hedwigia* 31:163–94.

Galinsky, E. A. 1995. Osmoadaptation in bacteria. *Adv. Microb. Physiol.* 37:274–328.

Garcia-Pichel, F. & Belnap, J. 1996. Microenviroements and microscale productivity of cyanobacterial desert crusts. *J. Phycol.* 32:774–82.

Garcia-Pichel, F. & Castenholz, R. W. 1994. On the significance of solar ultraviolet radiation for the ecology of microbial mats. *In* Stal, L. J. & Caumette, P. [Eds.] *Microbial Mats. Structure, Development and Environmental Significance* (NATO ASI Series, vol. 35). Springer-Verlag, Heidelberg, pp. 77–84.

Garcia-Pichel, F., Nübel, U. & Muyzer, G. 1998. The phylogeny of unicellular, extremely halotolerant cyanobacteria. *Arch. Microbiol.* 169:469–82.

Gerdes, G., Krumbein, W. E. & Holtkamp, E. 1985. Salinity and water activity related zonation of microbial communities and potential stromatolites of the Gavish Shabka. *In* Friedman, G. M. & Krumbein, W. E. [Eds.] *Hypersaline Ecosystems. The Gavish Shabka.* Springer-Verlag, New York, pp. 238–66.

Giani, D., Seeler, J., Giani, L. & Krumbein, W. E. 1989. Microbial mats and physicochemistry in a saltern in the Bretagne, France, and in a laboratory scale saltern model. *FEMS Microbiol. Ecol.* 62:151–62.

Javor, B. J. 1989. *Hypersaline Environments.* Springer Verlag, Berlin, 328 pp.

Javor, B. J. & Castenholz, R. W. 1984. Productivity studies in microbial mats, Laguna Guerrero Negro, Mexico. *In* Cohen, Y., Castenholz, R. W., & Halvorson, H. O. [Eds.]. *Microbial Mats: Stromatolites.* A R Liss, New York, pp. 149–70.

Jørgensen, B. B. & Cohen, Y. 1987. Photosynthetic potential and light-dependent oxygen consumption in a benthic cyanobacterial mat. *Appl. Environ. Microbiol.* 54:176–82.

Jørgensen, B. B. & Des Marais, D. J. 1990. The diffusive boundary layer of sediments: oxygen microgradients over a microbial mat. *Limnol. Oceanogr.* 35:1335–43.

Jørgensen, B. B. & Revsbech, N. P. 1985. Diffusive boundary layers and the oxygen uptake of sediments and detritus. *Limnol. Oceanogr.* 30:111–22.

Jørgensen, B. B., Revsbech, N. P. & Cohen, Y. 1983. Photosynthesis and structure of benthic microbial mats: microelectrode and SEM studies of four cyanobacterial communities. *Limnol. Oceanogr.* 28:1075–93.

Joset, F., Jeanjean, R., & Hagemann, M. 1996. Dynamics of the response of cyanobacteria to salt stress: deciphering the molecular events. *Physiol. Plant.* 96:738–44.

Kühl, M., Glud, R. N., Plough, H. & Ramsing, N. B. 1996. Microenvironmental control of photosynthesis and respiration and photosynthesis-coupled respiration in an epilithic cyanobacterial biofilm. *J. Phycol.* 32:799–812.

Li, Y.-H. and Gregory, S. 1974. Diffusion of ions in seawater and in deep-sea sediments. *Geochim Cosmochim Acta.* 38: 703–14.

Lorenzen, J., Glud, R. N., Revsech, N. P. 1995. Impact of microsensor-caused changes in diffusive boundary layer thickness on O_2 profiles and photosynthetic rates in benthic communities of microorganims. *Mar. Ecol. Prog. Ser.* 119:237–41.

Márquez, F. J., Sasaki, K., Nishio, N. & Nagai, S. 1995. Inhibitory effect of oxygen accumulation on the growth of *Spirulina platensis. Biotechnol. Lett.* 17:225–8.

Mir, J., Martínez-Alonso, M., Esteve, I. & Guerrero, R. 1991. Vertical stratification and microbial assemblage of a microbial mat in the Ebro Delta (Spain). *FEMS Microbiol. Ecol.* 86:59–68.

Nübel, U., Garcia-Pichel, F., Kühl, M. & Muyzer, G. 1999. Quantifying microbial diversity: morphotypes, 16S rRNA genes and carotenoids of oxygenic phototrophs in microbial mats. *Appl. Environm. Microbiol.* 65:422–30.

Pinckney, J., Paerl, H. W. & Bebout, B. M. 1995. Salinity control of benthic microbial mat community production in a Bahamian hypersaline lagoon. *J. Exp. Mar. Biol. Ecol.* 187:223–37.

Potts, M. 1980. Blue-green algae (Cyanophyta) in marine coastal environments of the Sinai peninsula: distribution, zonation, stratification and taxonomic diversity. *Phycologia* 19:60–73.

Raven, J. A. 1991. Implications of inorganic carbon utilization: ecology, evolution and geochemistry. *Can. J. Bot.* 69:908–24.

Revsbech, N. P. 1989. An oxygen microelectrode with a guard cathode. *Limnol. Oceanogr.* 34:474–8.

Revsbech, N. P. & Jørgensen, B. B. 1983. Photosynthesis of benthic microflora measured with high spatial resolution by the oxygen microprofile method: capabilities and limitations of the method. *Limnol. Oceanogr.* 28:749–56.

Revsbech, N. P., Jørgensen, B. B., Blackburn, T. H. & Cohen, Y. 1983. Microelectrode studies of the photosynthesis and O_2, H_2S and pH profiles of a microbial mat. *Limnol. Oceanogr.* 28: 1062–74.

Riley, J. P. 1975. *Chemical Oceanography, Vol 4.* Academic Press, London, p. 338.

Schopf, J. W. & Klein, C. [Eds.]. 1992. *The Proterozoic Biosphere. A Multidisciplinary Study.* Cambridge University Press, Cambridge, 1348 pp.

Schultze, L. S., Ferris, F. G., Sherwood, L. B. & Gerits, J. P. 1996. Ultrastructure and seasonal growth patterns of microbial mats in a temperate climate saline-alkaline lake: Goodenough Lake, Britisch Columbia, Canada. *Can. J. Microbiol.* 42: 147–61.

Sherwood, J. E., Stagnitti, F., Kokkin, J. & Williams, W. D. 1991. Dissolved oxygen concentrations in hypersaline waters. *Limnol. Oceanogr.* 36:325–50.

Vogel, S. 1989. *Life in Moving Fluids.* Princeton University Press, New Jersey, 532 pp.

Vonshak, A., Guy, R & Guy, M. 1988. The response of the filamentous cyanobacterium *Spirulina platensis* to salt stress. *Arch. Microbiol.* 150:417–20.

Wilson, S. E., Cumming, B. F., Smol, J. P. 1996. Assessing the reliability of salinity inference models from diatom assemblages: an examination of 219-lake data set from western North America. *Can. J. Fish. Aquat. Sci.* 53:1580–94.

Yopp, J. H., Tindall, D. R., Miller, D. M. & Schmidt, W. E. 1978. Isolation, purification and evidence for the halophilic nature of the blue-green alga *Aphanothece halophitica. Phycologia* 17: 172–8.

Zhang, Y. & Hoffmann, L. 1992. Blue-green algal mats of the salinas in San-Ya, Hai-nan Island (China): structure, taxonomic composition, and implications for the interpretation of Precambrian stromatolites. *Precambrian Res.* 56:275–90.